Published in final edited form as:
Langmuir. 2008 December 2; 24(23): 13250–13253. doi:10.1021/la802909c.

Evidence for Leaflet-Dependent Redistribution of Charged Molecules in Fluid Supported Phospholipid Bilayers

Andrew P. Shreve[1], **Michael C. Howland**[2], **Annapoorna R. Sapuri-Butti**[3], **Toby W. Allen**[4], and **Atul N. Parikh**[2,3]

1*Center for Integrated Nanotechnologies, Materials Physics and Applications Division, Los Alamos National Laboratory, Los Alamos, NM 87545*

2*Chemical Engineering and Materials Science, University of California, Davis, CA 95616*

3*Applied Science Department, University of California, Davis, CA 95616*

4*Chemistry Department, University of California, Davis, CA 95616*

Abstract

The asymmetric distribution of charged molecules between the leaflets of solid-substrate-supported phospholipid bilayers is studied using imaging ellipsometry, fluorescence microscopy, and numerical solutions of the Poisson-Boltzmann equation. Experiments are facilitated by the use of patterned substrates that allow for side-by-side comparison of lipid monolayers and supported bilayers. On silica surfaces, negatively charged lipid components are shown to be enriched in the outer leaflet of a supported bilayer system at modest salt concentrations. The approaches developed provide a general means for determining asymmetries of charged components in supported lipid bilayers.

Introduction

Supported membranes, single phospholipid bilayers, 4-6 nm in thickness, deposited on solid surfaces[1], are well-defined models for biological membranes. They are finding uses in areas ranging from fundamental biophysical investigations to biomimetic devices (e.g., biosensors)[2]. They may be formed by the fusion of unilamelar vesicles onto solid surfaces[3]. Typical support surfaces (e.g., silica) and many membrane constituents are electrically charged, so Coulombic interactions, unless offset by ions in solution, can induce stable compositional asymmetries. Indeed, several recent papers[4-6] have reported uneven interleaflet distribution of charged lipids for supported bilayers formed by vesicle fusion on charged substrates.

However, understanding remains poor of which experimental variables will allow reproducible control of asymmetries. Such control is crucial for many applications. For instance, asymmetric partitioning of charged lipid fluorophores or ligands may influence widely used fluorescence microscopy measurements[7] or skew analyses based on estimated densities of ligands in outer leaflets[8-10]. Further, better control over asymmetries in model substrate-supported systems may allow designing more complex model membranes that mimic interleaflet asymmetry and processes (e.g., flip-flop) in natural biological membranes[11, 12].

We present a simple experimental means to determine leaflet-dependent compositional asymmetry within supported membranes, and use numerical Poisson-Boltzmann methods to model the substrate/solution/membrane heterostructure. These methods lead to insights into the strength of interactions that influence partitioning of charged components, and also demonstrate a new strategy for measuring membrane asymmetries. Our approach uses patterned surfaces consisting of hydrophilic, negatively charged, and hydrophobic, electrically neutral, regions, on which isolated bilayers and phospholipid monolayers, respectively, can be

deposited[13]. Because both the monolayers and bilayers of large domains (~100 × 100 μm^2) are derived from the same small vesicle (~100 nm) source, they are expected to have identical overall lipid composition. Thus, the monolayer should present the vesicular composition, but the outer leaflet of the bilayers may present more (or less) of any given component, depending on the degree of asymmetry present. Thus, our use of patterned surfaces allows direct, side-by-side, determination of any enrichment (or depletion) of charged components in the outer leaflet of supported bilayers as compared to a monolayer reference. To measure such differences, we study protein binding to charged lipid receptors (gangliosides) and concentration dependent fluorescence resonance energy transfer (FRET) involving charged dye-labeled lipid acceptors, using imaging ellipsometry and quantitative fluorescence microscopy. The former technique, in particular, provides a label-free assessment of membrane structure and receptor binding[14].

Experimental Section

Materials

Fluorescein-5-isothiocyanate-labeled cholera toxin B5 sub-units (FITCCTB) and n-octadecyltricholorsilane (OTS) were purchased from Sigma-Aldrich. 1-palmitoyl-2-oleoyl-sn-glycero-3-phosphocholine (POPC), and monosialoganglioside (GM1) were purchased from Avanti Polar Lipids. Texas-red 1,2-dihexadecanoyl-sn-glycero-3-phosphoethanolamine (TRDHPE, as a triethyl ammonium salt) was purchased from Invitrogen.

Sample Preparation

Chemically patterned glass (or oxidized silicon) surfaces presenting negatively charged hydrophilic and neutral hydrophobic regions in predetermined geometries are produced by self-assembly of OTS, followed by photopatterning using short wavelength UV radiation[13]. Next, small, 110 nm diameter, unilamellar vesicles of POPC doped with 1 mol% GM1 are prepared and deposited onto these patterned substrates by vesicle fusion[9, 10]. Typically, vesicles are prepared by mechanical extrusion in water and the resulting vesicular solution adjusted with phosphate buffered saline (PBS) to produce the salt concentration of 75 mM. For certain samples, the ionic strength was adjusted by addition of sodium chloride. Lipid monolayers and bilayers are produced on the hydrophobic and hydrophilic regions, respectively. Importantly, previous studies have established that no diffusional communication occurs between lipids contained in the monolayer region and bilayer regions[13]. Two sets of samples are prepared, differentiated by the presence and absence of 1 mol% of negatively charged fluorescent TRDHPE. Subsequently, the samples are exposed to 1.7×10^{-7} M FITC-CTB, which binds selectively with GM1[15].

Imaging Ellipsometry

Imaging ellipsometry measurements were carried out using a commercial imaging ellipsometer (iElli2000, Nanofilm, Gottingen, Germany) operating at 532 nm with a custom-designed fluid cell. The angle of incidence was fixed at 60° and the 20 mW laser was operated at 6% power.

Fluorescence Microscopy

Fluorescence micrographs were taken on an inverted epifluorescence microscope (Nikon TE200E, Technical Instruments, San Francisco, USA), equipped with a high spatial resolution CCD camera.

Results and Discussion

Results from a typical sample, patterned as 100 μm squares, are presented in Figure 1. An ellipsometrically derived thickness map (Fig. 1a, 1c) indicates that the combined thickness of

the OTS and the phospholipid monolayer nearly matches that of the phospholipid bilayer. Because the OTS is ~2.6 nm in height, the observed thickness confirms our previous observations[13] that the lipid monolayer is structurally similar to that of the outer leaflet of the nearby bilayers. Following exposure to CTB, the thickness map (Fig. 1b, 1d) indicates ~2.5 times greater change in the thickness of the bilayer region relative to the monolayer region, consistent with higher CTB coverage. Control experiments without GM1 show no non-specific binding of CTB for these conditions. Both the monovalent interaction affinity and the cross-linking constant are known for the interaction of CTB with GM1, which may occur with up to penta-valent coordination of GM1[16]. Using these values, we estimate that our experiments should yield 30% and 60% monolayer coverage of CTB, for 1 mol% and 2 mol% GM1, respectively (for details of these estimates, see supporting information). Irrespective of these estimates, lack of complete monolayer coverage of CTB in either region implies a regime in which total binding of CTB increases with the presented density of GM1. Thus, ellipsometry results indicate that, at modest salt concentrations, GM1 is present in substantially higher concentration in the outer leaflet of the supported bilayer relative to the phospholipid monolayer. Deducing an ellipsometric thickness requires accurate knowledge of the refractive index of an effective uniform film, which is difficult to assess for sub-monolayer coverages. Thus, we also present support for higher CTB adsorption in the bilayer regions obtained using epifluorescence microscopy. The CTB is FITC labeled, and the resulting image (Fig. 1e), confirms a significantly higher emission from the bilayer regions of the sample. Since electrostatic interactions are mediated by salt concentration, we have also carried out a parallel series of studies at 10 × salt concentration. In this case, bilayers and monolayers show comparable amounts of CTB binding (Fig. 1h-1k).

Next, we explored the situation when the starting vesicles contain head-labeled, negatively charged, Texas-Red DHPE (1 mol%). TR-DPHE forms a FRET pair with FITC, with a Förster radius of ~5 nm[10]. With added TR-DHPE, red-channel fluorescence images strikingly illustrate the contrast between the phospholipid bilayer regions (Fig. 1f, bright squares) and the monolayer regions (Fig. 1f, dimmer surrounding regions). However, these images provide no information on the interleaflet distribution of TR-DHPE. To address this distribution, we note that epifluorescence images in the FITC channel (Fig. 1g) reveal markedly lower intensity for the bilayer regions, despite the greater amount of FITC-CTB known to be present in these regions (see above). The observed diminution in FITC fluorescence intensity indicates FRET-quenching due to TR-DHPE. A complete reversal of image contrast between the case with no TRDHPE (Fig.1e) and the case with 1 mol% TR-DHPE (Fig. 1g) implies significantly greater quenching of FITC by TR-DHPE in the supported bilayer region relative to the monolayer region. Based on the known Förster radius, there is expected to be no FRET between FITC bound to the exterior of one phospholipid leaflet and TRDHPE in the head-group region of the opposite leaflet, so these results report only on the outer leaflet density of the TR-DHPE. Thus, the contrast reversal observed between the two FITC images (Figs 1e and 1g) indicates that TR-DHPE is asymmetrically enriched in the outer leaflet of the bilayer.

Taken together, the experimental results indicate that the two negatively charged lipids (Texas-red DHPE and GM1) examined here, preferentially populate distal leaflets in bilayers on negatively charged substrates (e. g., silica) at modest salt concentrations. These results agree well with previous observations wherein much higher concentrations of negatively charged, phosphatidylserine (-PS) and positively charged, di- or trimethyl ammonium propane (-DAP or -TAP) have been shown to respond to substrate charges[4-6]. Our findings differ from a later study by Richter et al.[17] where they suggest that negatively charged PS lipids are evenly distributed on silica. This discrepancy can be explained by the relatively high ionic strength of the experiments in Richter et al. (see Figure 2 panel C below for details of this effect). Furthermore, the results illustrate generally useful experimental techniques for estimating interleaflet partitioning preferences of specific molecules. The experimental results likely

reflect electrostatic interactions[18], but steric effects arising from interaction of membrane components with the underlying substrate could also play a role in controlling asymmetry[19].

To further explore the role of electrostatic effects, we now turn to quantitative numerical calculations of the magnitude of electrostatic interactions. In our modeling (see supporting information), the silica substrate contains 3.3 negative unit charges per 100 Å^2 [20]. Interactions with these charges will be modulated by dielectric media and screened by ions in solution, as described by the Poisson-Boltzmann equation. For a planar charged interface, solutions obey Gouy-Chapman theory[21], which describes a decay in the electrostatic potential away from the surface governed by the Debye screening length. In 50 mM salt solution the screening length is ~14 Å whereas at 500 mM it is just ~4 Å. By comparison, the silica membrane separation distance has been variously estimated to be 10-20 Å[22-24].

However, Gouy-Chapman theory cannot be used to determine the potential difference across a membrane supported by the silica surface because the interactions with silica charges will be modulated by other dielectrics in the system. Most notably the membrane possesses a low dielectric hydrocarbon core that does not play host to ions, so there is no Debye screening in its interior. Furthermore one must consider the role of the silica slab beneath the charges; also a low dielectric (4.5) insulator. Non-linear Poisson-Boltzmann solutions were carried out for the supported membrane geometry illustrated in Fig. 2A. The water between the silica and the membrane is assumed, to a first approximation, to be bulk like, and electrolyte concentrations symmetric about the membrane. Also, while interactions between charged lipids become important at high charged lipid mole fractions, at the low lipid concentrations used here, the propensity for asymmetric distribution across the bilayer depends only on the electrostatic potential due to the silica substrate.

Traces shown in Fig. 2B reveal that at a high ionic concentration of 500 mM there is rapid screening of the potential due to the silica charges, but that at 50 mM the potential is still large at the lower membrane interface, resulting in a linear drop across the membrane (solid white curve) that creates a potential difference between the two interfaces. This potential difference will establish a gradient in the anionic lipid concentration across the membrane, favoring the top monolayer. As a comparison, the Gouy-Chapman solutions (dashed lines), predict erroneous screening through the membrane bilayer. The data shown in Fig. 2C show that this potential difference is a monotonically decreasing function of concentration in the range of 0 to 500mM, as presented in Figure 2B. The potential difference becomes significant (of the order of kT) for ionic strengths below 200 mM, depending slightly on the membrane-silica separation distance. These results suggest that experiments carried out at 75 mM should observe a large gradient of anionic lipids across the membrane, favoring the outer leaflet (by perhaps a factor of 5 based on a Boltzmann distribution), but that at 500 mM and above the effect may not even be noticeable. This prediction was confirmed in our experiments using 750 mM salt concentration (Fig. 1h-k), where we found no measurable preference for GM1 in the outer leaflet of supported bilayers.

These results indicate that for low salt concentrations, the potential energy difference for a negatively charged molecule in the inner vs. outer leaflets of supported lipid bilayers competes with thermal randomization and produces sustained asymmetry. The quantitative degree of enrichment is sensitive to several system-specific parameters, e.g., the actual position of the substrate charges relative to the membrane surface, substrate charge density, and the dielectric properties of the membrane (in part, determined by lipid composition). These calculations do, however, offer a simple means for predicting lipid asymmetries under various experimental conditions, and can be tested by systematic future experiments using the approaches presented above.

In summary, we have demonstrated a method based on the use of patterned, confined surface regions and quantitative imaging ellipsometry, with support from fluorescence microscopy, that confirms enrichment of negative components in outer leaflets of POPC membranes on silica surfaces at modest salt concentrations. The results of numerical Poisson-Boltzmann models confirm that electrostatic interactions provide an important enrichment mechanism. Overall, when charged components are involved, these results confirm a need for caution in quantitative interpretation of experiments that rely upon the use of, for example, particular values of receptor densities in outer leaflets of supported membranes.

Supplementary Material

Refer to Web version on PubMed Central for supplementary material.

Acknowledgements

Work at LANL and UCD was supported by the DOE Office of Science, Basic Energy Sciences, through the Biomolecular Materials Program (grant DE-FG02-04ER4613 at UCD). MCH and TWA are supported by NIH (T32-GM08799) and NSF (MCB-0546768), respectively.

References

1. Sackmann E. Supported membranes: Scientific and practical applications. Science 1996;271(5245): 43–48. [PubMed: 8539599]
2. Castellana ET, Cremer PS. Solid supported lipid bilayers: From biophysical studies to sensor design. Surface Science Reports 2006;61(10):429–444.
3. Tamm LK, McConnell HM. Supported Phospholipid-Bilayers. Biophysical Journal 1985;47(1):105–113. [PubMed: 3978184]
4. Kasbauer M, Junglas M, Bayerl TM. Effect of cationic lipids in the formation of asymmetries in supported bilayers. Biophysical Journal 1999;76(5):2600–2605. [PubMed: 10233074]
5. Richter RP, Maury N, Brisson AR. On the effect of the solid support on the interleaflet distribution of lipids in supported lipid bilayers. Langmuir 2005;21(1):299–304. [PubMed: 15620318]
6. Rossetti FF, Bally M, Michel R, Textor M, Reviakine I. Interactions between titanium dioxide and phosphatidyl serine-containing liposomes: Formation and patterning of supported phospholipid bilayers on the surface of a medically relevant material. Langmuir 2005;21(14):6443–6450. [PubMed: 15982052]
7. Boxer SG. Molecular transport and organization in supported lipid membranes. Current Opinion in Chemical Biology 2000;4(6):704–709. [PubMed: 11102877]
8. Moran-Mirabal JM, Edel JB, Meyer GD, Throckmorton D, Singh AK, Craighead HG. Micrometer-sized supported lipid bilayer arrays for bacterial toxin binding studies through total internal reflection fluorescence microscopy. Biophysical Journal 2005;89(1):296–305. [PubMed: 15833994]
9. Shi JJ, Yang TL, Kataoka S, Zhang YJ, Diaz AJ, Cremer PS. GM(1) clustering inhibits cholera toxin binding in supported phospholipid membranes. Journal of the American Chemical Society 2007;129 (18):5954–5961. [PubMed: 17429973]
10. Wong AP, Groves JT. Molecular topography imaging by intermembrane fluorescence resonance energy transfer. Proceedings of the National Academy of Sciences of the United States of America 2002;99(22):14147–14152. [PubMed: 12391328]
11. Gurtovenko AA, Vattulainen I. Molecular mechanism for lipid flip-flops. Journal of Physical Chemistry B 2007;111(48):13554–13559.
12. Rothman JE, Lenard J. Membrane Asymmetry. Science 1977;195(4280):743–753. [PubMed: 402030]
13. Howland MC, Sapuri-Butti AR, Dixit SS, Dattelbaum AM, Shreve AP, Parikh AN. Phospholipid morphologies on photochemically patterned silane monolayers. Journal of the American Chemical Society 2005;127(18):6752–6765. [PubMed: 15869298]

14. Howland MC, Szmodis AW, Sanii B, Parikh AN. Characterization of physical properties of supported phospholipid membranes using imaging ellipsometry at optical wavelengths. Biophysical Journal 2007;92(4):1306–1317. [PubMed: 17142265]

15. Holmgren J, Lonnroth I, Mansson JE, Svennerholm L. Interaction of Cholera Toxin and Membrane Gm1 Ganglioside of Small-Intestine. Proceedings of the National Academy of Sciences of the United States of America 1975;72(7):2520–2524. [PubMed: 1058471]

16. Lauer S, Goldstein B, Nolan RL, Nolan JP. Analysis of cholera toxin-ganglioside interactions by flow cytometry. Biochemistry 2002;41(6):1742–1751. [PubMed: 11827518]

17. Richter RP, Him JLK, Tessier B, Tessier C, Brisson AR. On the kinetics of adsorption and two-dimensional self-assembly of annexin A5 on supported lipid bilayers. Biophysical Journal 2005;89 (5):3372–3385. [PubMed: 16085777]

18. Langner M, Kubica K. The electrostatics of lipid surfaces. Chemistry and Physics of Lipids 1999;101 (1):3–35. [PubMed: 10810922]

19. Victorov AV, Janes N, Taraschi TF, Hoek JB. Packing constraints and electrostatic surface potentials determine transmembrane asymmetry of phosphatidylethanol. Biophysical Journal 1997;72(6): 2588–2598. [PubMed: 9168034]

20. Iler, RK. The Chemistry of Silica: Solubility, Polymerization, Colloid and Surface Properties and Biochemistry of Silica. Wiley-Interscience; 1979.

21. Israelachvili, J. Intermolecular and Surface Forces. Vol. 2. Academic Press; London: 1992. p. 450

22. Kiessling V, Tamm LK. Measuring distances in supported bilayers by fluorescence interference-contrast microscopy: Polymer supports and SNARE proteins. Biophysical Journal 2003;84(1):408–418. [PubMed: 12524294]

23. Koenig BW, Kruger S, Orts WJ, Majkrzak CF, Berk NF, Silverton JV, Gawrisch K. Neutron reflectivity and atomic force microscopy studies of a lipid bilayer in water adsorbed to the surface of a silicon single crystal. Langmuir 1996;12(5):1343–1350.

24. Miller CE, Majewski J, Gog T, Kuhl TL. Characterization of biological thin films at the solid-liquid interface by X-ray reflectivity. Physical Review Letters 2005;94(23)

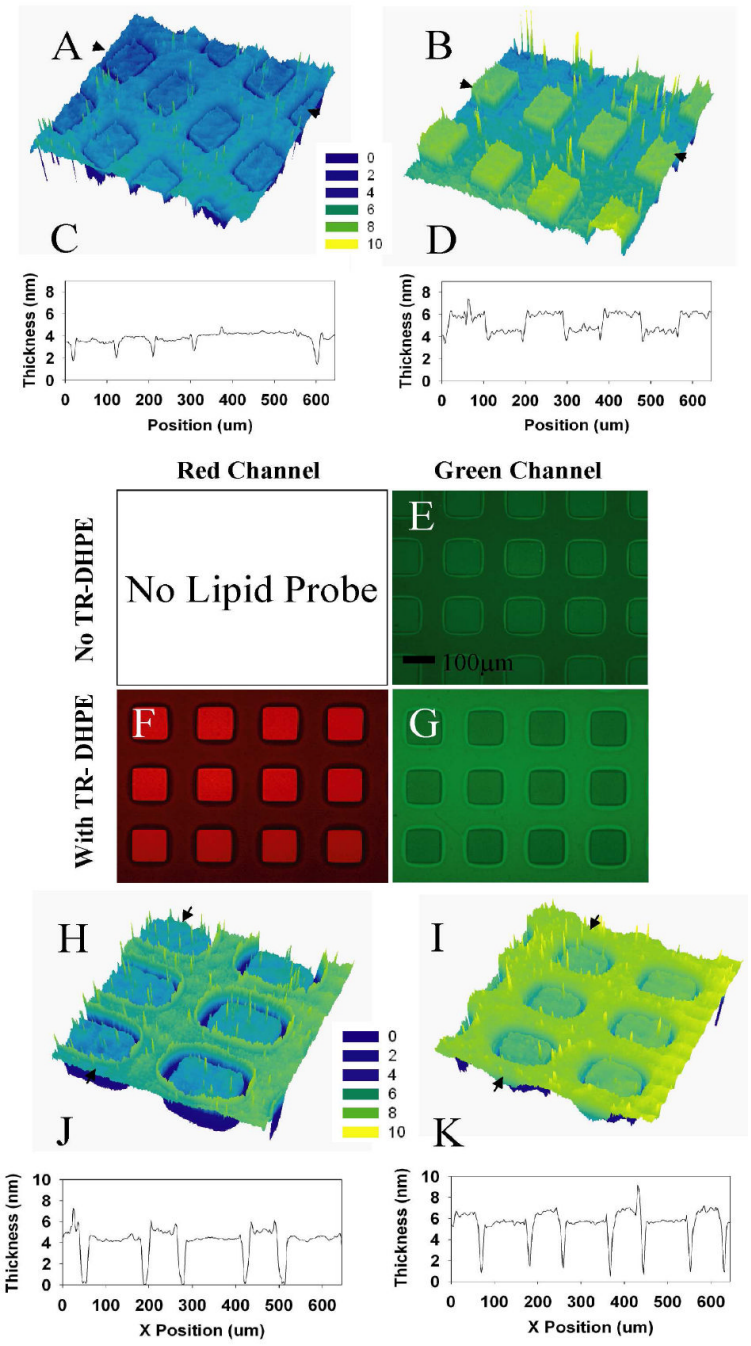

Figure 1.

(a) Ellipsometric thickness map of a mono- and bilayer pattern consisting of 1 mol % GM1 99 mol % POPC in 75 mM PBS medium and (c) a corresponding line scan for a linear region between the arrows in (a). Panels (b) and (d) show the ellipsometric profiles for the same sample after incubation with FITC labeled cholera toxin B-subunits. (e) Epifluorescence image of an identical companion sample on glass revealing FITC (green channel.) emission due to CTB adsorption. (f, g) Epifluorescence images showing the red (Texas-red DHPE emission) and green channel (FITC-CTB emission) fluorescence patterns of a comparable sample doped with 1 mol % texas-red labeled DHPE lipid after incubation with FITC-CTB. The principal membrane constituents are 1 mol % GM1, and 98 mol % POPC. (h) Ellipsometric thickness

map of the mono/bilayer lipid pattern consisting of 1 mol % GM1 99mol % POPC at 750 mM PBS and (j) corresponding line scan as indicated by arrows in (h). Panels (i) and (k) show the elliposometric profiles for the same sample after incubation with CTB.

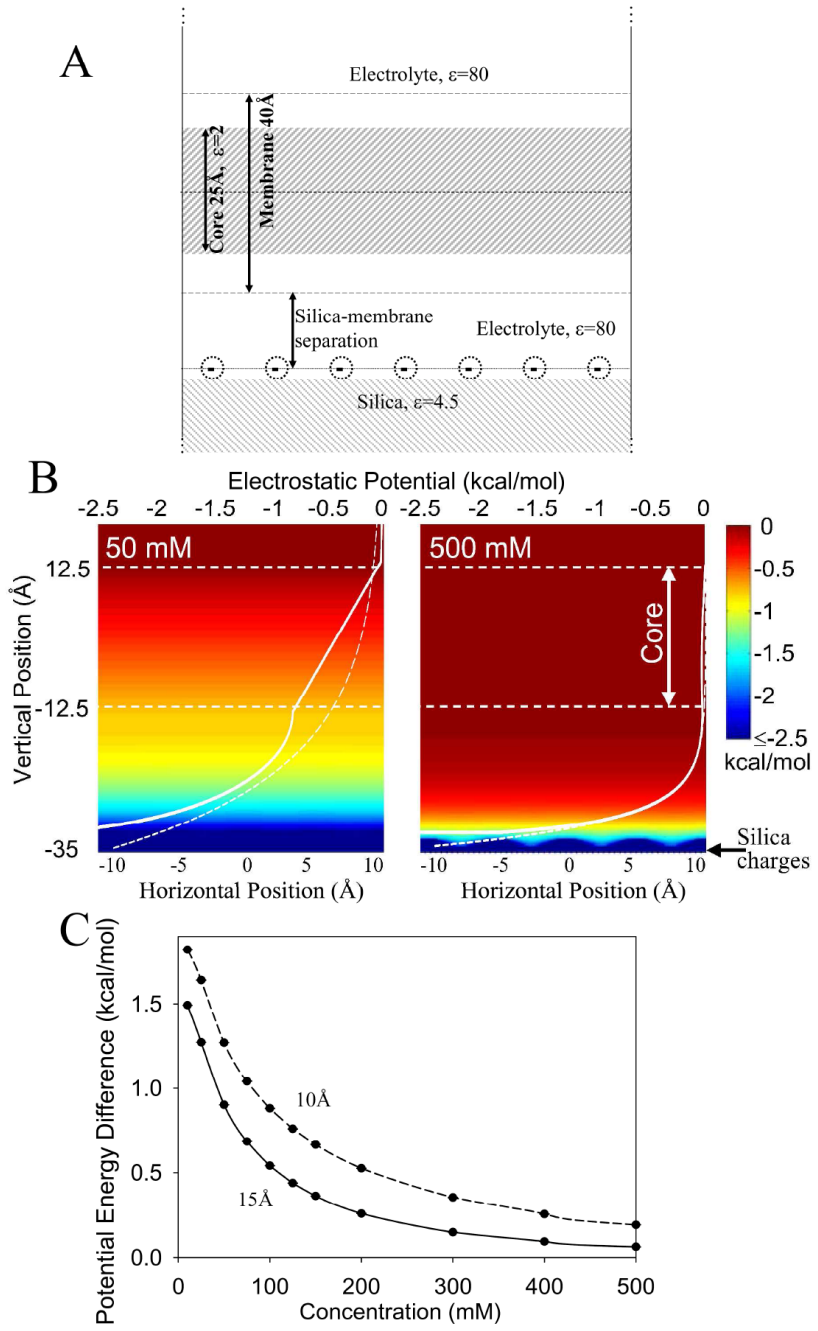

Figure 2.

(a) The model consists of a 40 Å thick membrane surrounded by a symmetric 1:1 electrolyte above a silica slab. The silica slab, coated with a 2D periodic lattice of negative silanol charges, was placed 10 or 15 Å below the lower membrane interface. (b) Potential maps as a function of distance parallel (horizontal axis) and normal (vertical axis) to the membrane surface for 50 and 500 mM monovalent salt solutions for a silica-membrane separation of 15 Å. Superimposed on these maps are 1D plots of the potential (white solid curves, upper horizontal axes) as well as the corresponding Gouy-Chapman results as dashed white curves. (c) The salt concentration dependence of the potential energy difference between the two interfaces of the membrane for membrane-silica separations of 10 Å and 15 Å.